Title: Imaging Tumour Hypoxia with Positron Emission Tomography

Running title: Imaging Tumour Hypoxia with PET

Authors:

Ian N. Fleming[1], PhD

Roido Manavaki[2], PhD

Philip J. Blower[3], DPhil, CChem, FRSC

Catharine West[4], PhD

Kaye J. Williams[5, 8], PhD

Adrian L. Harris[6], FMedSci, FRCP

Juozas Domarkas[7], PhD

Simon Lord[6], MD

Claire Baldry[3], MD

Fiona J. Gilbert[2, 8], FRCR, FRCP ([***])

Affiliations:

[1]Aberdeen Biomedical Imaging Centre, Lilian Sutton Building, Foresterhill, Aberdeen, AB25 2ZD, UK

[2]Department of Radiology, School of Clinical Medicine, University of Cambridge, Box 218 - Cambridge Biomedical Campus, Cambridge, CB2 0QQ, UK

[3]Division of Imaging Sciences and Biomedical Engineering, 4th Floor, Lambeth Wing, St. Thomas' Hospital, King's College London, London, SE1 7EH, UK

[4]Institute of Cancer Sciences, Manchester Academic Health Science Centre, University of Manchester, Wilmslow Road, Manchester M20 4BX, UK

[5]Manchester Pharmacy School, Faculty of Medical and Human Sciences, University Manchester, Stopford Building, Oxford Road, Manchester, M13 9PT, UK

[6]Molecular Oncology Laboratories, University Department of Medical Oncology, The Weatherall Institute of Molecular Medicine, University of Oxford, John Radcliffe Hospital, Headington, Oxford, OX3 9DS, UK

[7]Centre for Cardiovascular & Metabolic Research, Respiratory Medicine, Hull-York Medical School, University of Hull, Hull, HU16 5JQ, UK

[8]EPSRC & CRUK Cancer Imaging Centre in Cambridge and Manchester, UK

[***] *Corresponding Author*

Manuscript type: Review

Corresponding author:

Professor Fiona J. Gilbert,

Department of Radiology,

School of Clinical Medicine,

University of Cambridge

Box 218 | Cambridge Biomedical Campus

Cambridge, CB2 0QQ

UK

Email: fjg28@medschl.cam.ac.uk

Telephone No: + 44 (0)1223 746439;

Fax No: +44 (0)1223 330915

Abstract

Hypoxia, a hallmark of most solid tumours, is a negative prognostic factor due to its association with an aggressive tumour phenotype and therapeutic resistance. Given its prominent role in oncology, accurate detection of hypoxia is important, as it impacts on prognosis and could influence treatment planning. A variety of approaches have been explored over the years for detecting and monitoring changes in hypoxia in tumours, including biological markers and non–invasive imaging techniques. Positron emission tomography (PET) is the preferred method for imaging tumour hypoxia due to its high specificity and sensitivity to probe physiological processes *in vivo*, as well as the ability to provide information about intracellular oxygenation levels. This review provides an overview of imaging hypoxia with PET, with an emphasis on the advantages and limitations of the currently available hypoxia radiotracers.

Introduction

Low oxygen concentration (hypoxia) is associated with many human pathological processes including ischemic heart disease, stroke and cancer. In oncology, hypoxic tumours are associated with a poor prognosis, an aggressive phenotype, increased risk of invasion and metastasis, and resistance to chemo and radiation therapy. A practical, robust and reproducible method of detecting and quantifying hypoxia could improve patient outcomes by allowing selection of more appropriate therapies to overcome the effects of hypoxia or allowing stratification of patients for more accurate prognostic information.

Tumour hypoxia has been studied with various techniques: oxygen electrodes; extrinsic (e.g. pimonidazole) and intrinsic (e.g. carbonic anhydrase IX, CAIX) biomarkers; blood oxygen level–dependent (BOLD) and tissue oxygen level–dependent (TOLD) magnetic resonance imaging (MRI); single photon emission computed tomography (SPECT) and positron emission tomography (PET). Each technique interrogates different aspects of the hypoxic microenvironment, as they provide information on hypoxia at different locations: PET, SPECT and extrinsic markers, report on intracellular hypoxia (although not specifically inside cell nuclei and PET/SPECT images quantify data on a macroscopic scale in tumour regions), BOLD–MRI allows assessment of blood oxygenation using deoxy-haemoglobin as an endogenous marker, while oxygen electrodes, OxyLite sampling and electron paramagnetic resonance (EPR) predominantly measure interstitial hypoxia. Indirect methods that report on hypoxia–induced molecular events (e.g. GLUT1, CAIX expression) rather than hypoxia itself have also been employed as markers of tumour oxygenation. PET displays some advantages for studying hypoxia, as it can employ radiotracer probes that directly report on oxygen levels, in principle permitting the non-invasive and three–dimensional assessment

of intratumour oxygen levels in a more direct manner, and not via hypoxia–mediated changes in phenotype.

Due to the clinical significance of hypoxia imaging, an increasing number of hypoxia PET tracers are being evaluated in the clinic. This review provides a summary and discussion of tumour hypoxia imaging with PET, emphasising the attributes and limitations of the currently available hypoxia radiotracers.

The significance of tumour hypoxia

Tissue hypoxia is the result of inadequate tissue oxygenation due to an imbalance between oxygen supply and consumption. Hypoxia in solid tumours is largely due to the decreased delivery of oxygenated blood to meet the increased metabolic demands of the rapidly proliferating tumour cells. Other pathogenetic factors pre–eminent in the aetiology of tumour hypoxia lie in the chaotic and primitive tumour microvasculature which exhibits severe structural and functional abnormalities, heterogeneous microcirculation patterns, and an adverse geometry which poses limitations to oxygen diffusion. In addition, the reduced oxygen binding ability and/or transport capacity of haemoglobin, due to rouleaux formation, and the presence of disease– or therapy–related anaemia may also exacerbate hypoxia (Vaupel and Harison, 2004).

Tumour hypoxia may be broadly classified as chronic and acute. Chronic or diffusion–limited hypoxia primarily arises as a consequence of the disorganised vascular architecture of tumours, where the distances between tumour microvessels are often increased from normal. Consequently, the diffusion distances of oxygen in perivascular space – typically 70–180 μm from the nearest capillary – are often exceeded. In addition, an adverse vascular geometry and prolonged reductions in blood oxygen content due to anaemia can also result in chronic

hypoxia. By contrast, acute or perfusion–limited hypoxia is characterised by fluctuations in tumour blood flow that are caused by transient reductions in perfusion. Both chronic and acute hypoxia can concur in tumours, leading to the formation of a highly dynamic microenvironment, where cells are exposed to differential oxygen gradients both spatially and temporally (Vaupel and Harrison, 2004). Owing to the dynamic and heterogeneous character of tumour hypoxia, imaging with PET presents an attractive alternative, as it does not require invasive biopsies, provides information across the entire tumour, and allows repeated and quantifiable measurements.

Hypoxia has been shown to change gene expression to favour survival in a hostile environment (Bristow and Hill, 2008). The cellular response to hypoxia is mainly controlled by the family of hypoxia–inducible factors (HIFs), and may involve regulation of up to 1·5% of the human genome. HIF–1 – the best characterised member of the HIF family – is a heterodimeric protein, consisting of an oxygen responsive α–subunit and a constitutively expressed β–subunit. In the presence of oxygen, HIF–1α is continuously synthesised and degraded, but in hypoxic conditions, the protein accumulates, heterodimerises and acts as a transcription factor to up regulate a multitude of genes, including those involved in glucose metabolism, pH regulation, apoptosis, cell survival under oxidative stress, angiogenesis and erythropoiesis (Semenza, 2004). These characteristics eventually confer tumours with resistance to chemoradiation therapy and higher degrees of invasiveness. Furthermore, hypoxia itself reduces free radical formation induced by radiation, providing a physical contribution to resistance. Several retrospective immunohistochemical studies have demonstrated that hypoxia–mediated expression of HIF–1α and its downstream genes (e.g. glucose transporter 1, GLUT–1; vascular endothelial factor, VEGF; CAIX) is a negative prognostic indicator for many cancer types (Jubb *et al*, 2010). Treatment resistance to radio

and chemotherapy has also been demonstrated. Radiotherapy relies on the formation of free radicals which cause DNA damage; a mechanism that is enhanced in the presence of oxygen. Chemotherapeutic resistance may also be explained by a multitude of mechanisms, including extracellular acidification, resistance to apoptosis and increased genomic instability. Consequently, patients with hypoxic tumours often have a poor prognosis and decreased overall survival rate.

Measuring tumour hypoxia with PET

Radionuclide detection of hypoxia in tumours was first reported in 1981 with ^{14}C–misonidazole autoradiography (Chapman, 1979). Subsequently, two main tracer classes have been developed to specifically study hypoxia with PET: ^{18}F–labelled nitroimidazoles and Cu–labelled diacetyl–bis(N^4–methylthiosemicarbazone) analogues (Figure 1).

From a PET imaging perspective, hypoxia markers need to exhibit a number of different properties. The tracer must readily and non–specifically enter cells, sample the intracellular milieu, and leave cells only in the presence of relevant oxygen concentrations. A summary of the attributes of the ideal hypoxia tracer is presented in Table 1. Most PET tracers tested clinically broadly display attributes 1, 4, 5 and 7. The clinical utility of each tracer depends on these key properties, which will influence its distribution in tissues, clearance rate from blood, normoxic and hypoxic cells, metabolism, optimal image acquisition time and ease of synthesis, distribution.

Nitroimidazole analogues

2–nitroimidazole compounds were originally developed as hypoxic cell radiosensitisers and were introduced as hypoxia markers in the 1970's (Chapman *et al*, 1979). Nitroimidazoles

enter cells by passive diffusion, where they undergo reduction forming a reactive intermediate species. Under normoxic conditions, these molecules are re–oxidised into their parent compound and diffuse out of the cell. However hypoxia causes further reduction of the nitro–radical anion, which eventually becomes irreversibly trapped in the cell at rates that are inversely proportional to the local pO_2. As reduction of nitroimidazoles requires the presence of active tissue reductases, these compounds accumulate within viable hypoxic cells, but not apoptotic or necrotic cells.

^{18}F–FMISO: Over the years, several fluorinated nitroimidazole–based markers have been developed for PET imaging. Of these, ^{18}F–fluoromisonidazole (^{18}F–FMISO) constitutes the prototype 2–nitroimidazole tracer, and is the most extensively clinically studied PET hypoxia biomarker. The lipophilic nature of this compound ensures facile cell–membrane penetration and diffusion into tissue, and several studies correlating direct oxygen measurements with ^{18}F–FMISO accumulation *in vivo* demonstrate that a median oxygen level of ≤10 mmHg is generally required for hypoxia–specific retention. ^{18}F–FMISO accumulation has been found to reflect hypoxia in gliomas (Valk *et al*, l992; Bruehlmeier *et al*, 2004; Rajendran *et al*, 2004; Cher *et al* 2006; Swanson *et al* 2009), head–and–neck (Rasey *et al*, 1996; Gagel *et al*, 2004, 2007; Hicks *et al*, 2005; Thorwarth *et al*, 2006; Zimny *et al*, 2006; Mortensen *et al*, 2010; Abolmaali *et al*, 2011; Sato *et al*, 2013), breast (Cheng *et al*, 2013), lung (Cherk *et al*, 2006; Vera *et al*, 2011) and renal tumours (Hugonet *et al*, 2011). However, ^{18}F–FMISO retention in sarcomas is variable (Rajendran *et al*, 2003; Mortensen *et al*, 2010), rectal ^{18}F–FMISO imaging is compromised by high non–specific tracer accumulation in normoxic tissue (Roels *et al*, 2008) whereas no retention was observed in pancreatic tumours (Segard *et al*, 2013). Several clinical studies have shown that a tumour–to–blood activity ratio ≥ 1.2 imaged after at least two hours post injection (p.i.) can be generally considered as indicative

of hypoxia (Table 2). Although not commercially available, ^{18}F–FMISO is produced by a number of institutions, making it available for research purposes.

Due to its hypoxic selectivity, ^{18}F–FMISO is the lead candidate in the assessment of hypoxia with PET. However, despite its wide applicability, ^{18}F–FMISO has not gained general acceptance for routine clinical use due to its slow pharmacokinetic profile: the limited clearance of the tracer from normal tissue and blood results in modest hypoxic–to–normoxic tissue ratios (Fig 2) and therefore images with moderate contrast (Fig 3a). The limited hypoxic contrast may potentially impede visual detection of hypoxic regions, and has hampered diagnostic utility in routine practice. Therefore, considerable efforts have been made to develop hypoxia markers with improved pharmacokinetic properties (enhanced clearance of the tracer from normoxic tissues) that are more amenable to clinical use. These are discussed below.

^{18}F–FAZA: ^{18}F–fluoroazomycin–arabinofuranoside (^{18}F–FAZA) is more hydrophilic than ^{18}F–FMISO. Consequently, there are faster clearance kinetics, resulting in improved tumour–to–reference tissue ratios, and thus hypoxia–to–normoxia contrast. ^{18}F–FAZA imaging has been successful in gliomas (Postema *et al*, 2009), lymphomas (Postema *et al*, 2009), lung (Postema *et al*, 2009; Bollineni *et al*, 2013; Trinkaus *et al*, 2013), head–and–neck (Postema *et al*, 2009; Souvatzoglou *et al*, 2007; Grosu *et al*, 2007; Mortensen *et al* 2012), cervical (Schuetz *et al*, 2010) and rectal tumours (Havelund *et al*, 2013), and results have been shown to compare favourably with equivalent ^{18}F–FMISO data, especially as improved hypoxic–normoxic contrast was obtained at earlier time–points. No ^{18}F–FAZA accumulation has been observed in prostate tumours, although hypoxia may not be a characteristic of this particular tumour type, as in the same study, CAIX immunohistochemistry was also found to be negative in these lesions (Garcia-Parra *et al*, 2011). High ^{18}F–FAZA tumour–to–reference

tissue values have been associated with reduced disease–free survival and have shown prognostic potential in the detection of hypoxia in head–and–neck patients (Mortensen *et al*, 2012). Due to the higher tumour–to–reference tissue ratios in comparison to ^{18}F–FMISO, ^{18}F–FAZA is gaining popularity for PET imaging of tumour hypoxia. Despite the fact that ^{18}F–FAZA is not widely available at present, increasing research demand may persuade more sites to produce it.

^{18}F–FETNIM: ^{18}F–fluoroerythronitroimidazole (^{18}F–FETNIM) studies in head–and–neck (Lehtiö *et al*, 2001, 2003), lung (Li *et al*, 2010; Hu *et al*, 2013) and oesophageal cancer Yue *et al*, 2012 calculated T:M in the range of 1.4–2.48 at two hours p.i. High tumour–to–muscle values were found to be indicative of reduced progression–free and overall survival in lung (Hu *et al*, 2013), head–and–neck (Lehtiö *et al*, 2001) oesophageal (Yue *et al*, 2012), and cervical (Vercellino *et al* 2012). Clinical studies with ^{18}F–FETNIM have been mainly carried out at the University of Turku, Finland. ^{18}F–FETNIM is not being used at present in the UK or the USA.

^{18}F–RP–170: More recently, RP–170 (1–(2–1–(1H–methyl)ethoxy)methyl–2–nitroimidazole), another 2–nitroimidazole–based hypoxic radiosensitiser, has also been labelled with [18]F. The hypoxic selectivity of ^{18}F–FRP–170 was demonstrated in glioma patients on the basis of significant correlations between uptake, oxygen tension measurements and HIF–1α immunostaining (Beppu *et al*, 2014). Studies in brain (Shibahara *et al*, 2010; Beppu *et al*, 2014) and lung (Kaneta *et al*, 2007) tumours indicated higher SUV for hypoxic than normal tissues; tumour–to–reference tissue ratio of 1.7 were calculated at one hour p.i., which could be clinically sufficient for assessing hypoxia. The shorter interval

prior to scanning, combined with improved hypoxic contrast compared to ^{18}F–FMISO, suggests that ^{18}F–FRP–170 could potentially be useful in the clinic.

^{18}F–HX4:   [18]F–3–fluoro–2–(4–((2–nitro–1H–imidazol–1–yl)methyl)–1H–1,2,3–triazol–1–yl)propan–1–ol (^{18}F–HX4) contains a 1,2,3–anti–triazole moiety (as a synthetic convenience) rendering it more hydrophilic than ^{18}F–FMISO. In head–and–neck tumours ^{18}F–HX4 produced tumour–to–reference tissue values similar to ^{18}F–FMISO at relatively early time points p.i., indicating the potential advantage of shorter acquisition times (Chen *et al,* 2012). However a more recent study in non–small–cell lung cancer (NSCLC) patients (Zegers *et al*, 2013) suggested that later scan times (2–4 hrs p.i.) can further enhance the hypoxic–to–normoxic signal. In all of the above tracers the more accurate hypoxic measure is made at least two hours post injection, but the trade–off is the reduced radioactivity and noisier data.

Cu–ATSM

An alternative class of agents for the study of hypoxia with PET is based on a complex of Cu with diacetyl–bis(N^4–methylthiosemicarbazone) ligands, among which diacetyl–bis(N^4–methylthiosemicarbazone) (ATSM) is the prototype. Due to its lipophilicity and low molecular weight, Cu–ATSM is characterised by high membrane permeability and therefore rapid diffusion into cells. The hypoxic specificity of Cu–ATSM is thought to be partly imparted by the intra–cellular reduction of Cu(II) to Cu(I) combined with re–oxidation by intra–cellular molecular oxygen. Under hypoxic conditions, the unstable Cu(I)–ATSM complex may further dissociate into Cu(I) and ATSM, leading to the intra–cellular trapping of the Cu(I) ion. In the presence of oxygen, the [Cu(I)–ATSM]⁻ can be re–oxidised to its parent compound, allowing efflux from the cell (Dearling and Packard, 2010) .

Tumour–specific Cu–ATSM retention has been demonstrated for head–and–neck (Minagawa *et al*, 2011; Nyflot *et al*, 2012) (Fig 3b), lung (Takahashi *et al*, 2000; Dehdashti *et al*, 2003; Lolith *et al*, 2009), cervical (Dehdashti *et al*, 2003; Grisby *et al*, 2007; Lewis *et al*, 2008; Dehdashti *et al*, 2008), rectal tumours (Dietz *et al*, 2008) and gliomas (Tateishi *et al*, 2013). Hypoxia specificity may be dependent on tumour type: preclinical studies showed good correlation in the intra–tumour distribution of Cu–ATSM and ^{18}F–FMISO in a FaDu squamous carcinoma model but not at early time points in an R3327–AT anaplastic rat prostate tumour (O'Donoghue *et al*, 2005). A recent study has raised concerns about the hypoxic specificity of Cu–ATSM, as hepatic metabolism of the compound results in images that reflect the behaviour of ionic Cu (uptake of which may itself be hypoxia–related) rather than Cu–ATSM itself, especially at later time points (1–24 hrs) (Hueting *et al*, 2014). Of concern is also the fact that while some preclinical studies show that tumour uptake of hypoxia–selective Cu–ATSM analogues (e.g. Cu–ATSE) decreases with increased oxygenation (McQuade *et al*, 2005), another report showed that increased oxygenation resulted in a decrease in uptake of FMISO, but not of Cu–ATSM (Matsumoto *et al*, 2007). Nevertheless, ^{64}Cu–ATSM retention has been shown to correlate clinically with poor prognosis (Dehdashti *et al*, 2003, 2008; Grisby *et al*, 2007; Dietz *et al* 2008). Attempts to investigate the relationship between the intra–tumoural distribution of Cu–ATSM with histological and other hypoxia markers have also yielded both positive and negative correlations. Although it appears to be premature to reject Cu–ATSM on the grounds of hypoxic non–specificity, further studies are required to elucidate the *in vivo* behaviour of this tracer to allow for better interpretation of the imaging information. The development of second generation Cu–ATSM analogues, with reduced lipophilicity and improved hypoxia selectivity and sensitivity, appear a promising alternative to Cu–ATSM (Handley *et al*, 2014). Cu–ATSM has several potential advantages relative to other tracers for the imaging of

tumour hypoxia, including simpler synthesis/radiolabelling methodology and faster clearance from normoxic tissues, which allows shorter intervals between injection and imaging and higher hypoxic–to–normoxic contrast. Notwithstanding the limited availability of Cu isotopes, ^{64}Cu–ATSM is currently being produced at a few research sites, and due to the 12 hour half–life could potentially be utilised for clinical studies.

Clinical applications of PET hypoxia imaging

Identification of tumour hypoxia and prediction of prognosis/response to treatment

Identifying individuals with poor prognosis and those likely to benefit from hypoxia–targeted therapy are important objectives of PET hypoxia research. Several studies have shown that PET hypoxia imaging can provide information on prognosis. High ^{18}F–FMISO retention has been associated with higher risk of loco–regional failure and shorter progression–free survival in head–and–neck (Rischin *et al*, 2006; Rajendran *et al*, 2006; Thorwarth *et al*, 2006; Dirix *et al*, 2009; Lee *et al*, 2009; Kikuchi *et al*, 2011) and renal cancer (Hugonet *et al*, 2011). Furthermore, a meta–review of the clinical data of over 300 patients concluded that FMISO is a predictor of poor treatment response and prognosis (Lee and Scott, 2007). Similar results have been reported for ^{18}F–FETNIM in lung (Li *et al*, 2010), head–and–neck (Lehtiö *et al*, 2004), and oesophageal cancer (Yue *et al*, 2012), where high tumour–to–reference tissue values were also associated with poor patient outcomes. Studies conducted with ^{18}F–FAZA in squamous cell carcinomas of the head and the neck (Mortensen *et al*, 2012) and Cu–ATSM in patients with cervical (Dehdashti *et al*, 2003; Grigsby *et al*, 2007), lung (Dehdashti *et al*, 2003) and rectal cancer (Dietz *et al*, 2008) have also demonstrated that lower tumour–to–muscle ratios are indicative of better prognosis, progression–free and overall survival. A meta–analysis of published PET hypoxia studies has demonstrated a common tendency towards poorer outcome in tumours showing higher tracer accumulation (Horsman *et al*, 2012). Decreased ^{18}F–FMISO uptake in response to radio– or chemotherapy

has been reported in brain (Swanson *et al*, 2009), head–and–neck (Yamane *et al*, 2011; Eschmann *et al*, 2007), lung (Koh *et al*, 1995; Gagel *et al*, 2006), and renal tumours (Hugonet *et al*, 2011); although some studies did not observe an analogous decrease with response to therapy (Thorwarth *et al*, 2006; Vera *et al*, 2011). Decreased tumour–to–muscle ratios signifying full or partial response to chemotherapy have also been obtained with Cu–ATSM in lung (Dehdashti *et al*, 2003) and head–and–neck tumours (Minagawa *et al*, 2011), and ^{18}F–FAZA in lung cancer (Trinkaus *et al*, 2013).

Radiotherapy planning

In oncology, there is interest in the identification of intra–tumoural areas with hypoxia to guide radiation dose escalation to radio–resistant sub–volumes. Despite possible limitations associated with the reproducibility of hypoxic volume measurements (temporal changes and/or heterogeneity in the spatial distribution of intra–tumoural hypoxia), the biological information from PET hypoxia scans is being explored for the identification and delineation of hypoxic areas within the tumour mass for dose escalation. Modern radiation techniques, such as intensity modulated radiotherapy (IMRT) or image–guided radiotherapy (IGRT) can help with radiotherapy planning (Horsmann *et al*, 2012). "Dose painting" by numbers, where a higher radiation dose is selectively delivered to areas of biological resistance identified either before or during the treatment course, has also been suggested (Geets *et al*, 2013). The feasibility of dose escalation to hypoxic sub–volumes has been primarily investigated in cancers of the head and neck, lung, and brain, and demonstrated with Cu–ATSM (Chao *et al*, 2001), ^{18}F–FMISO (Lee *et al*, 2008), and ^{18}F–FAZA (Grosu *et al*, 2007). Despite the fact that the majority of the aforementioned studies have not been conducted on actual patients, but on anthropomorphic phantoms (*in silico*) (Richin *et al*, 2006; Grosu *et al*, 2007; Lee *et al*, 2008)

, dose escalation on the basis of PET hypoxia imaging appears feasible, and further studies are required to investigate whether this can translate into clinical benefit.

Hypoxia therapeutics

As the hypoxic microenvironment constitutes a unique characteristic of tumours, hypoxia can also be harnessed as a therapeutic target. The main strategies for targeting hypoxia involve hypoxic cell radiosensitisers (e.g. nimorazole), hypoxic cell cytotoxins (e.g. tirapazamine, TH–302, PR–104A); and altering oxygen delivery (e.g. carbogen plus nicotinamide). Other approaches being investigated include hypoxia–selective gene therapy, altering metabolic pathways essential for survival under stress, and inhibitors of molecular targets activated in hypoxia (e.g. HIF–1) (Wilson and Hay, 2011). Imaging hypoxia with PET could facilitate the development of therapeutic agents by identifying patients with hypoxic tumours, and measuring response to hypoxia–modifying treatments providing a basis for individualising hypoxia–specific treatment, and/or assessing drug efficacy. Furthermore, it will allow development of new predictors and answer key questions, such as the relation of baseline or induced hypoxia to response to anti–angiogenic drugs and the relation of baseline hypoxia to response to hypoxic activated toxins. Such studies should be incorporated into trials of these agents routinely, to develop the necessary validation for their utility. This would greatly help the personalised and economic use of such therapies, which will be even more important if used in combination, e.g. anti–angiogenics and hypoxia–activated toxins. The potential of PET hypoxia imaging in directing hypoxia therapeutics has been clinically demonstrated with tirapazamine with ^{18}F–FMISO in head and neck tumours, whereby only those with hypoxia benefited from bioreductive drugs (Richin *et al*, 2006; Overgaard *et al*, 2011).

Considerations

1. The "ideal" PET tracer for tumour hypoxia

Table 3 presents a summary of clinical imaging findings with the hypoxia tracers discussed in this review. None of the currently available tracers have all the properties that constitute the ideal PET hypoxia tracer, and therefore none is optimal for imaging hypoxia in all cancer types. Nevertheless, the feasibility of imaging hypoxia with PET has been clinically demonstrated in various tumour entities using several of the existing radiotracers. Much of the radiotracer selection stems from the availability of the tracer, ease of synthesis and the tumour type.

2. The magnitude of the challenge of PET hypoxia imaging

A challenging aspect of PET hypoxia imaging is the fact that hypoxic tumours are often hypoperfused. Limited perfusion will restrict effective delivery of tracer into the tissue often, influencing tracer accumulation in regions of normal or tumour tissue, and often yielding results that are complex to interpret. Several studies have compared tumour perfusion with dynamic PET to ascertain whether tracer accumulation reflects blood flow during imaging. ^{18}F–FMISO (Bruehlmeier *et al*, 2004), ^{18}F–FETNIM (Lehtiö *et al*, 2001) and ^{18}F–FAZA (Shi *et al*, 2010) exhibited similar distribution patterns to $[^{15}O]$–H_2O PET (reflecting blood flow) up to 15 min p.i., while different patterns were observed at later imaging times, consistent with tracer accumulation in hypoxic regions. Pharmacokinetic analysis of ^{18}F–FMISO data suggests that different hypoxia–perfusion profiles can be identified in tumours (Thorwarth *et al*, 2005); the latter perhaps corresponding with the heterogeneity observed in tumour hypoxia distribution patterns (Grosu *et al*, 2007). The significant heterogeneity of the tumour microenvironment in terms of perfusion and hypoxia necessitates further clinical studies, not only to evaluate hypoxia–perfusion patterns, but also their relationship to clinical outcome.

3.   Validation of PET hypoxia measurements

Validation of PET tracers as indicators of regional hypoxia is extremely challenging and attempts to correlate PET images with other accepted hypoxia markers have produced mixed and contradictory results. While oxygen electrodes are considered to be the gold standard against which PET hypoxia measurements are authenticated, comparisons may yield several discrepancies due to the sampling limitations of oxygen probes and the fact that it measures hypoxia in a different location (interstitial for oxygen probes vs. intracellular for PET), as well as the fact that this technique will fail to distinguish between necrotic and viable hypoxic tissue (Höckel *et al*, 1993). This may partly explain results from several studies that have reported mixed correlations between tracer uptake and oxygen electrode measurements in various tumour types (Bentzen *et al*, 2003; Gagel *et al*, 2004, 2007; Zimny *et al*, 2006; Mortensen *et al*, 2010). Indirect immunohistochemical methods based on the detection of exogenous (e.g. pimonidazole, EF5) or endogenous hypoxia markers (e.g. CAIX, HIF–1) have also been employed (Dehdashti *et al*, 2003; Jubb *et al*, 2010), albeit with limited success. This is primarily due to the fact that comparisons as such rely on reproducible staining, and several representative biopsies (which are not always available), and may often require a technically challenging spatial co–registration between PET images with immunohistochemistry photographs for analogies to be drawn. Of note is the fact that although tracer accumulation has been widely compared with pimonidazole staining preclinically (Dubois *et al*, 2004), equivalent clinical comparisons have not yet been performed. The differential detection of acute and chronic hypoxia and the discrepancy between hypoxia at the microscopic level and the macroscopic resolution of the PET voxel are factors that will also limit the accuracy of such comparisons (Mortensen *et al*, 2010)

4.   Reproducibility of PET hypoxia measurements

Validation of the reproducibility of PET hypoxia measurements is also particularly important for clinical applications. There are limited clinical data available on scan reproducibility with PET hypoxia biomarkers. Studies with ^{18}F–FMISO in head–and–neck cancer reported reproducible hypoxic volumes in PET scans performed three days apart, but a considerable degree of intra–tumoural spatial variability in tracer accumulation (Nehmeh *et al*, 2008). Another study with ^{18}F–FMISO in lung cancer showed good inter-observer reproducibility on the basis of visual analysis, but low inter–observer agreement with respect to hypoxic volume measurements (Thureau *et al*, 2013). A more recent ^{18}F–FMISO study in head–and–neck cancer reported high reproducibility in SUV and tumour–to–reference tissue measurements in scans acquired two days apart (Okamoto *et al*, 2013). Other than ^{18}F–FMISO, a study with ^{18}F–FETNIM in oesophageal cancer patients observed similar uptake values between scans performed on separate days before concurrent chemoradioatherapy, but a shift in the geographical location of hypoxic regions (Yue *et al*, 2012). These heterogeneous findings can be partly explained by the dynamic character of hypoxia that will limit scan reproducibility. Although acute hypoxia has been shown to minimally influence ^{18}F–FMISO PET imaging in simulations (Mönnich *et al*, 2012), a study in head–and–neck tumours that used sequential ^{18}F–FMISO scans to distinguish between regions of acute and chronic hypoxia, accounted for 14–52% of acute hypoxia (Wang *et al*, 2009); a percentage that is comparable to the proportion of acute hypoxia measured in rodent tumours. Methodological discrepancies (scan setup, image acquisition protocol), the selection of hypoxic–to–normoxic thresholds for the definition of hypoxic regions, the temporal variability in intra–tumoural pO_2 levels between consecutive measurements, as well as the small number of patients in the majority of the studies may also account for the observed disparities in reproducibility. Further studies addressing the variability of PET hypoxia measurements are warranted, so as to clarify uncertainties in tumour hypoxia quantification.

Conclusions

As a number of PET hypoxia tracers have now been evaluated in cancer patients, it is apparent that PET imaging can be a powerful tool to identify hypoxia in the clinical setting. Although none of the currently available tracers exhibit all of the properties of the 'ideal' hypoxia tracer or are optimal for imaging hypoxia in all tumour types, studies have demonstrated the feasibility for imaging hypoxia in various cancers. As the clinical utility and limitations of PET hypoxia biomarkers are now being elucidated the process will be facilitated by performing larger studies with these tracers using standardised protocols and hypoxia definitions so as to improve comparison between tracers in various tumour types. This may be best achieved via inter-institutional collaborations which should help to advance study designs and homogeneous data reporting. Equally important are the performance of test–retest studies, harmonisation of data reporting, and clinical validation of hypoxia tracers. These key objectives must be addressed before PET hypoxia tracers can be used to their full clinical utility.

Search strategy and selection criteria

We searched PubMed and Scopus using combinations of the following search terms: "tumor hypoxia", "oncology", "PET", "positron emission tomography", radiotherapy", "nitroimidazoles", "fluoromisonidazole", "pimonidazole", "FMISO", "FAZA", "FETNIM", "FRP–170", "HX4", "Cu–ATSM". The search results were screened for relevance and the reference lists of relevant publications were also surveyed. PubMed and Scopus article recommendations were also examined for relevance. Only papers published in English were considered. The final reference list was compiled by considering papers published between January 1973 and May 2014.

Conflicts of interest

The authors declare that they have no conflicts of interest.

References

Abolmaali N, Haase R, Koch A, Zips D, Steinbach J, Baumann M, Kotzerke J, Zöphel K (2011) Two or four hour [^{18}F]FMISO–PET in HNSCC: When is the contrast best? *Nuklearmedizin* **50**(1): 22–7.

Bentzen L, Keiding S, Nordsmark M, Falborg L, Hansen SB, Keller J, Nielsen OS, Overgaard J (2003) Tumour oxygenation assessed by ^{18}F–fluoromisonidazole PET and polarographic needle electrodes in human soft tissue tumours. *Radiother Oncol* **67**(3): 339–44.

Beppu T, Terasaki K, Sasaki T, Fujiwara S, Matsuura H, Ogasawara K, Sera K, Yamada N, Uesugi N, Sugai T, Kudo K, Sasaki M, Ehara S, Iwata R, Takai Y (2014) Standardized

Uptake Value in High Uptake Area on Positron Emission Tomography with ^{18}F–FRP170 as a Hypoxic Cell Tracer Correlates with Intratumoral Oxygen Pressure in Glioblastoma. *Mol Imaging Biol* **16**(1): 1–9.

Bollineni VR, Kerner GSMA, Pruim J, Steenbakkers RJ, Wiegman EM, Koole MJ, de Groot EH, Willemsen AT, Luurtsema G, Widder J, Groen HJ, Langendijk JA (2013) PET imaging of tumor hypoxia using ^{18}F–fluoroazomycin arabinoside in stage III–IV non–small cell lung cancer patients. *J Nucl Med* **54**(8): 1175–80.

Bristow RG, Hill RP (2008) Hypoxia and metabolism: Hypoxia, DNA repair and genetic instability. *Nat Rev Cancer* **8**(3): 180–92.

Bruehlmeier M, Roelcke U, Schubiger PA, Ametamey SM (2004) Assessment of hypoxia and perfusion in human brain tumors using PET with ^{18}F–fluoromisonidazole and ^{15}O–H2O. *J Nucl Med*; **45**(11): 1851–9.

Chao KSC, Bosch WR, Mutic S, Lewis JS, Dehdashti F, Mintun MA, Dempsey JF, Perez CA, Purdy JA, Welch MJ (2001) A novel approach to overcome hypoxic tumor resistance: Cu–ATSM–guided intensity–modulated radiation therapy. *Int J Radiat Oncol Biol Phys* **49**(4): 1171–82.

Chapman JD (1979) Hypoxic sensitisers – Implications for radiation therapy. *N Engl J Med* **301**(26): 1429–32.

Chen L, Zhang Z, Kolb HC, Walsh JC, Zhang J, Guan Y (2012) ^{18}F–HX4 hypoxia imaging with PET/CT in head and neck cancer: A comparison with ^{18}F–FMISO. *Nucl Med Commun* **33**(10): 1096–102.

Cheng J, Lei L, Xu J, Sun Y, Zhang Y, Wang X, Pan L, Shao Z, Zhang Y, Liu G (2013) ^{18}F–fluoromisonidazole PET/CT: A potential tool for predicting primary endocrine therapy resistance in breast cancer. *J Nucl Med* **54**(3): 333–40.

Cher LM, Murone C, Lawrentschuk N, Ramdave S, Papenfuss A, Hannah A, O'Keefe GJ, Sachinidis JI, Berlangieri SU, Fabinyi G, Scott AM (2006) Correlation of hypoxic cell fraction and angiogenesis with glucose metabolic rate in gliomas using ^{18}F–fluoromisonidazole, ^{18}F–FDG PET, and immunohistochemical studies. *J Nucl Med* 2006 **47**(3): 410–8.

Cherk MH, Foo SS, Poon AMT, Knight SR, Murone C, Papenfuss AT, Sachinidis JI, Saunder TH, O'Keefe GJ, Scott AM (2006) Lack of correlation of hypoxic cell fraction and angiogenesis with glucose metabolic rate in non–small cell lung cancer assessed by ^{18}F–fluoromisonidazole and ^{18}F–FDG PET. *J Nucl Med* **47**(12): 1921–26.

Dearling JLJ, Packard AB (2010) Some thoughts on the mechanism of cellular trapping of Cu(II)–ATSM. *Nucl Med Biol* **37**(3): 237–43.

Dehdashti F, Grigsby PW, Mintun MA, Lewis JS, Siegel BA, Welch MJ (2003) Assessing tumor hypoxia in cervical cancer by positron emission tomography with [60]Cu–ATSM: Relationship to therapeutic response – A preliminary report. *Int J Radiat Oncol Biol Phys* **55**(5): 1233–8.

Dehdashti F, Mintun MA, Lewis JS, Bradley J, Govindan R, Laforest R, Welch MJ, Siegel BA (2003) In vivo assessment of tumor hypoxia in lung cancer with [60]Cu–ATSM. *Eur J Nucl Med Mol Imaging*; **30**(6): 844–50.

Dehdashti F, Grigsby PW, Lewis JS, Laforest R, Siegel BA, Welch MJ (2008) Assessing tumor hypoxia in cervical cancer by PET with [60]Cu–labeled diacetyl–bis(N4–methylthiosemicarbazone). *J Nucl Med* **49**(2): 201–5.

Dietz DW, Dehdashti F, Grigsby PW, Malyapa RS, Myerson RJ, Picus J, Ritter J, Lewis JS, Welch MJ, Siegel BA (2008) Tumor hypoxia detected by positron emission tomography with [60]Cu–ATSM as a predictor of response and survival in patients undergoing neoadjuvant chemoradiotherapy for rectal carcinoma: A pilot study. *Dis Colon Rectum* **51**(11): 1641–8.

Dirix P, Vandecaveye V, De Keyzer F, Stroobants S, Hermans R, Nuyts S (2009) Dose painting in radiotherapy for head and neck squamous cell carcinoma: Value of repeated functional imaging with ^{18}F–FDG PET, ^{18}F–fluoromisonidazole PET, diffusion–weighted MRI, and dynamic contrast–enhanced MRI. *J Nucl Med* **50**(7): 1020–7.

Dubois L, Landuyt W, Haustermans K, Dupont P, Bormans G, Vermaelen P, Flamen P, Verbeken E, Mortelmans L (2004) Evaluation of hypoxia in an experimental rat tumour model by [^{18}F]Fluoromisonidazole PET and immunohistochemistry. *Br J Cancer* **91**(11): 1947–54.

Eschmann SM, Paulsen F, Bedeshem C, Machulla HJ, Hehr T, Bamberg M, Bares R (2007) Hypoxia–imaging with ^{18}F–Misonidazole and PET: Changes of kinetics during radiotherapy of head–and–neck cancer. *Radiother Oncol* **83**(3): 406–10.

Gagel B, Reinartz P, DiMartino E, Zimny M, Pinkawa M, Maneschi P, Stanzel S, Hamacher K, Coenen HH, Westhofen M, Büll U, Eble MJ (2004) pO2 polarography versus positron emission tomography ([^{18}F] fluoromisonidazole, [^{18}F]–2–fluoro–2′– deoxyglucose): An appraisal of radiotherapeutically relevant hypoxia. *Strahlenther Onkol* **180**(10): 616–22.

Gagel B, Reinartz P, Demirel C, Kaiser HJ, Zimny M, Piroth M, Pinkawa M, Stanzel S, Asadpour B, Hamacher K, Coenen HH, Buell U, Eble MJ (2006) [^{18}F]–fluromisonidazole and [^{18}F] fluorodeoxyglucose positron emission tomography in response evaluation after chemo–/radiotherapy of non–small–cell lung cancer: A feasibility study. *BMC Cancer* **6**: 51.

Gagel B, Piroth M, Pinkawa M, Reinartz P, Zimny M, Kaiser HJ, Stanzel S, Asadpour B, Demirel C, Hamacher K, Coenen HH, Scholbach T, Maneschi P, DiMartino E, Eble MJ (2007) pO polarography, contrast enhanced color duplex sonography (CDS), [^{18}F] fluoromisonidazole and [^{18}F] fluorodeoxyglucose positron emission tomography: Validated methods for the evaluation of therapy–relevant tumor oxygenation or only bricks in the puzzle of tumor hypoxia? *BMC Cancer* **7**: 113.

Garcia–Parra R, Wood D, Shah RB, Siddiqui J, Hussain H, Park H, Desmond T, Meyer C, Piert M (2011) Investigation on tumor hypoxia in resectable primary prostate cancer as demonstrated by ^{18}F–FAZA PET/CT utilizing multimodality fusion techniques. *Eur J Nucl Med Mol Imaging* 2011; 1–8.

Geets X, Grégoire V, Lee JA (2013) Implementation of hypoxia PET imaging in radiation therapy planning. *Q J Nucl Med Mol Imaging* **57**(3): 271–82.

Grigsby PW, Malyapa RS, Higashikubo R, Schwarz JK, Welch MJ, Huettner PC, Dehdashti F (2007) Comparison of molecular markers of hypoxia and imaging with 60Cu–ATSM in cancer of the uterine cervix. *Mol Imaging Biol* **9**(5): 278–83.

Grosu AL, Souvatzoglou M, Röper B, Dobritz M, Wiedenmann N, Jacob V, Wester HJ, Reischl G, Machulla HJ, Schwaiger M, Molls M, Piert M (2007) Hypoxia Imaging With FAZA–PET and Theoretical Considerations With Regard to Dose Painting for

Individualization of Radiotherapy in Patients With Head and Neck Cancer. *Int J Radiat Oncol Biol Phys* **69**(2): 541–51.

Handley MG, Medina RA, Mariotti E, Mariotti E, Kenny GD, Shaw KP, Yan R, Eykyn TR, Blower PJ, Southworth R. (2014) Cardiac hypoxia imaging: Second–generation analogues of ^{64}Cu–ATSM. *J Nucl Med* **55**(3): 488–94.

Havelund BM, Holdgaard PC, Rafaelsen SR, Mortensen LS, Theil J, Bender D, Pløen J, Spindler KL, Jakobsen A (2013) Tumour hypoxia imaging with ^{18}F–fluoroazomycinarabinofuranoside PET/CT in patients with locally advanced rectal cancer. *Nucl Med Commun* **34**(2): 155–61.

Hicks RJ, Rischin D, Fisher R, Binns D, Scott AM, Peters LJ (2005) Utility of FMISO PET in advanced head and neck cancer treated with chemoradiation incorporating a hypoxia–targeting chemotherapy agent. *Eur J Nucl Med Mol Imaging* **32**(12): 1384–91.

Höckel M, Knoop C, Schlenger K, Vorndran B, Baussmann E, Mitze M, Knapstein PG, Vaupel P (1993) Intratumoral pO2 predicts survival in advanced cancer of the uterine cervix. *Radiother Oncol* **26**(1): 45–50.

Horsman MR, Mortensen LS, Petersen JB, Busk M, Overgaard J (2012) Imaging hypoxia to improve radiotherapy outcome. *Nat Rev Clin Oncol* **9**(12): 674–87.

Hu M, Xing L, Mu D, Yang W, Yang G, Kong L, Yu J (2013) Hypoxia imaging with ^{18}F–fluoroerythronitroimidazole integrated PET/CT and immunohistochemical studies in non–small cell lung cancer. *Clin Nucl Med* **38**(8): 591–6.

Hueting R, Kersemans V, Cornelissen B, Tredwell M, Hussien K, Christlieb M, Gee AD, Passchier J, Smart SC, Dilworth JR, Gouverneur V, Muschel RJ (2014) A comparison of the behavior of ^{64}Cu–acetate and ^{64}Cu–ATSM in vitro and in vivo. *J Nucl Med* **55**(1): 128–34.

Hugonnet F, Fournier L, Medioni J, Smadja C, Hindié E, Huchet V, Itti E, Cuenod CA, Chatellier G, Oudard S, Faraggi M; Hypoxia in Renal Cancer Multicenter Group (2011) Metastatic renal cell carcinoma: Relationship between initial metastasis hypoxia, change after 1 month's sunitinib, and therapeutic response: An ^{18}F–fluoromisonidazole PET/CT study. *J Nucl Med* **52**(7): 1048–55.

Jubb AM, Buffa FM, Harris AL (2010) Assessment of tumour hypoxia for prediction of response to therapy and cancer prognosis. *J Cell Mol Med* **14**(1–2): 18–29.

Kaneta T, Takai Y, Iwata R, Hakamatsuka T, Yasuda H, Nakayama K, Ishikawa Y, Watanuki S, Furumoto S, Funaki Y, Nakata E, Jingu K, Tsujitani M, Ito M, Fukuda H, Takahashi S, Yamada S (2007) Initial evaluation of dynamic human imaging using ^{18}F–FRP170 as a new PET tracer for imaging hypoxia. *Ann Nucl Med* **21**(2): 101–7.

Kikuchi M, Yamane T, Shinohara S, Fujiwara K, Hori SY, Tona Y, Yamazaki H, Naito Y, Senda M (2011) ^{18}F–fluoromisonidazole positron emission tomography before treatment is a predictor of radiotherapy outcome and survival prognosis in patients with head and neck squamous cell carcinoma. *Ann Nucl Med* **25**(9): 625–33.

Koh WJ, Bergman KS, Rasey JS, Peterson LM, Evans ML, Graham MM, Grierson JR, Lindsley KL, Lewellen TK, Krohn KA, Griffin TW (1995) Evaluation of oxygenation status during fractionated radiotherapy in human nonsmall cell lung cancers using [F–18]fluoromisonidazole positron emission tomography. *Int J Radiat Oncol Biol Phys* 1995; **33**(2): 391–8.

Lee NY, Mechalakos JG, Nehmeh S, Lin Z, Squire OD, Cai S, Chan K, Zanzonico PB, Greco C, Ling CC, Humm JL, Schöder H (2008) Fluorine–18–Labeled Fluoromisonidazole Positron Emission and Computed Tomography–Guided Intensity–Modulated Radiotherapy for Head and Neck Cancer: A Feasibility Study. *Int J Radiat Oncol Biol Phys* **70**(1): 2–13.

Lee N, Nehmeh S, Schöder H, Fury M, Chan K, Ling CC, Humm J (2009) Prospective Trial Incorporating Pre–/Mid–Treatment [18F]–Misonidazole Positron Emission Tomography for Head–and–Neck Cancer Patients Undergoing Concurrent Chemoradiotherapy. *Int J Radiat Oncol Biol Phys* **75**(1): 101–8.

Lee ST, Scott AM (2007) Hypoxia Positron Emission Tomography Imaging With 18F–Fluoromisonidazole. *Semin Nucl Med* **37**(6): 451–61.

Lehtiö K, Oikonen V, Grönroos T, Eskola O, Kalliokoski K, Bergman J, Solin O, Grénman R, Nuutila P, Minn H (2001) Imaging of blood flow and hypoxia in head and neck cancer: Initial evaluation with [15O]H2O and [18F]Fluoroerythronitroimidazole PET. *J Nucl Med* **42**(11): 1643–52.

Lehtiö K, Oikonen V, Nyman S, Grönroos T, Roivainen A, Eskola O, Minn H (2003) Quantifying tumour hypoxia with fluorine–18–fluoroerythronitroimidazole ([18F]FETNIM) and PET using the tumour to plasma ratio. *Eur J Nucl Med Mol Imaging* **30**(1): 101–8.

Lehtiö K, Eskola O, Viljanen T, Oikonen V, Grönroos T, Sillanmäki L, Grénman R, Minn H (2004). Imaging perfusion and hypoxia with PET to predict radiotherapy response in head–and–neck cancer. *Int J Radiat Oncol Biol Phys* **59**(4): 971–82.

Lewis JS, Laforest R, Dehdashti F, Grigsby PW, Welch MJ, Siegel BA (2008) An imaging comparison of 64Cu–ATSM and 60Cu–ATSM in cancer of the uterine cervix. *J Nucl Med* **49**(7): 1177–82.

Li L, Hu M, Zhu H, Zhao W, Yang G, Yu J (2010) Comparison of ^{18}F–fluoroerythronitroimidazole and ^{18}F–fluorodeoxyglucose positron emission tomography and prognostic value in locally advanced non–small–cell lung cancer. *Clin Lung Cancer* **11**(5): 335–40.

Lohith TG, Kudo T, Demura Y, Umeda Y, Kiyono Y, Fujibayashi Y, Okazawa H (2009) Pathophysiologic correlation between [62]Cu–ATSM and ^{18}F–FDG in lung cancer. *J Nucl Med* **50**(12): 1948–53.

Matsumoto K, Szajek L, Krishna MC, Cook JA, Seidel J, Grimes K, Carson J, Sowers AL, English S, Green MV, Bacharach SL, Eckelman WC, Mitchell JB (2007) The influence of tumor oxygenation on hypoxia imaging in murine squamous cell carcinoma using [^{64}Cu]Cu-ATSM or [^{18}F]Fluoromisonidazole positron emission tomography. *Int J Oncol* **30**(4): 873–81.

McQuade P, Martin KE, Castle TC, Went MJ, Blower PJ, Welch MJ, Lewis JS (2005) Investigation into ^{64}Cu–labeled Bis(selenosemicarbazone) and Bis(thiosemicarbazone) complexes as hypoxia imaging agents. *Nucl Med Biol* **32**(2): 147–56.

Minagawa Y, Shizukuishi K, Koike I, Horiuchi C, Watanuki K, Hata M, Omura M, Odagiri K, Tohnai I, Inoue T, Tateishi U (2011) Assessment of tumor hypoxia by [62]Cu–ATSM PET/CT as a predictor of response in head and neck cancer: A pilot study. *Ann Nucl Med* **25**(5): 339–45.

Mönnich D, Troost EGC, Kaanders JHAM, Oyen WJG, Alber M, Thorwarth D (2012) Modelling and simulation of the influence of acute and chronic hypoxia on [^{18}F]fluoromisonidazole PET imaging. *Phys Med Biol* **57**(6): 1675–84.

Mortensen LS, Buus S, Nordsmark M, Bentzen L, Munk OL, Keiding S, Overgaard J (2010) Identifying hypoxia in human tumors: A correlation study between ^{18}F–FMISO PET and the Eppendorf oxygen–sensitive electrode. *Acta Oncol* **49**(7): 934–40.

Mortensen LS, Johansen J, Kallehauge J, Primdahl H, Busk M, Lassen P, Alsner J, Sørensen BS, Toustrup K, Jakobsen S, Petersen J, Petersen H, Theil J, Nordsmark M, Overgaard J (2012) FAZA PET/CT hypoxia imaging in patients with squamous cell carcinoma of the head and neck treated with radiotherapy: Results from the DAHANCA 24 trial. *Radiother Oncol* **105**(1): 14–20.

Nehmeh SA, Lee NY, Schröder H, Squire O, Zanzonico PB, Erdi YE, Greco C, Mageras G, Pham HS, Larson SM, Ling CC, Humm JL (2008) Reproducibility of Intratumor Distribution of ^{18}F–Fluoromisonidazole in Head and Neck Cancer. *Int J Radiat Oncol Biol Phys*; **70**(1): 235–42.

Nyflot MJ, Harari PM, Yip S, Perlman SB, Jeraj R (2012) Correlation of PET images of metabolism, proliferation and hypoxia to characterize tumor phenotype in patients with cancer of the oropharynx. *Radiother Oncol* **105**(1): 36–40.

O'Donoghue JA, Zanzonico P, Pugachev A, Wen B, Smith-Jones P, Cai S, Burnazi E, Finn RD, Burgman P, Ruan S, Lewis JS, Welch MJ, Ling CC, Humm JL (2005) Assessment of regional tumor hypoxia using ^{18}F–fluoromisonidazole and ^{64}Cu(II)–diacetyl–bis(N4–methylthiosemicarbazone) positron emission tomography: Comparative study featuring

microPET imaging, pO_2 probe measurement, autoradiography, and fluorescent microscopy in the R3327–AT and FaDu rat tumor models. *Int J Radiat Oncol Biol Phys* **61**(5): 1493–502.

Okamoto S, Shiga T, Yasuda K, Ito YM, Magota K, Kasai K, Kuge Y, Shirato H, Tamaki N (2013) High reproducibility of tumor hypoxia evaluated by [18]F– fluoromisonidazole pet for head and neck cancer. *J Nucl Med* **54**(2): 201–7.

Overgaard J (2011) Hypoxic modification of radiotherapy in squamous cell carcinoma of the head and neck – A systematic review and meta–analysis. *Radiother Oncol* **100**(1): 22–32.

Postema EJ, McEwan AJB, Riauka TA, Kumar P, Richmond DA, Abrams DN, Wiebe LI (2009) Initial results of hypoxia imaging using 1–α–d–(5–deoxy–5–[^{18}F]– fluoroarabinofuranosyl)–2–nitroimidazole (^{18}F–FAZA). *Eur J Nucl Med Mol Imaging* **36**(10): 1565–73.

Rajendran JG, Wilson DC, Conrad EU, Peterson LM, Bruckner JD, Rasey JS, Chin LK, Hofstrand PD, Grierson JR, Eary JF, Krohn KA (2003) [^{18}F]FMISO and [^{18}F]FDG PET imaging in soft tissue sarcomas: Correlation of hypoxia, metabolism and VEGF expression. *Eur J Nucl Med and Molecular Imaging* **30**(5): 695–704.

Rajendran JG, Mankoff DA, O'Sullivan F, Peterson LM, Schwartz DL, Conrad EU, Spence AM, Muzi M, Farwell DG, Krohn KA (2004) Hypoxia and Glucose Metabolism in Malignant Tumors: Evaluation by [^{18}F]Fluoromisonidazole and [^{18}F]]Fluorodeoxyglucose Positron Emission Tomography Imaging. *Clin Cancer Res* **10**(7): 2245–52.

Rajendran JG, Schwartz DL, O'Sullivan J, Peterson LM, Ng P, Scharnhorst J, Grierson JR, Krohn KA (2006) Tumor hypoxia imaging with [F–18] fluoromisonidazole positron emission tomography in head and neck cancer. *Clin Cancer Res* **12**(18): 5435–41.

Rasey JS, Koh WJ, Evans ML, Peterson LM, Lewellen TK, Graham MM, Krohn KA (1996) Quantifying regional hypoxia in human tumors with positron emission tomography of [^{18}F]fluoromisonidazole: A pretherapy study of 37 patients. *Int J Radiat Oncol Biol Phys* **36**(2): 417–28.

Rischin D, Hicks RJ, Fisher R, Binns D, Corry J, Porceddu S, Peters LJ (2006) Prognostic significance of [^{18}F]–misonidazole positron emission tomography–detected tumor hypoxia in patients with advanced head and neck cancer randomly assigned to chemoradiation with or without tirapazamine: A substudy of Trans–Tasman Radiation Oncology Group study 98.02. *J Clin Oncol* **24**(13): 2098–104.

Roels S, Slagmolen P, Nuyts J, Lee JA, Loeckx D, Maes F, Stroobants S, Penninckx F, Haustermans K (2008) Biological image–guided radiotherapy in rectal cancer: Is there a role for FMISO or FLT, next to FDG? *Acta Oncol* **47**(7): 1237–48.

Sato J, Kitagawa Y, Yamazaki Y, Hata H, Okamoto S, Shiga T, Shindoh M, Kuge Y, Tamaki N (2013) ^{18}F–fluoromisonidazole PET uptake is correlated with hypoxia–inducible factor–1a expression in oral squamous cell carcinoma. *J Nucl Med* **54**(7): 1060–5.

Schuetz M, Schmid MP, Pötter R, Kommata S, Georg D, Lukic D, Dudczak R, Kletter K, Dimopoulos J, Karanikas G, Bachtiary B (2010) Evaluating repetitive ^{18}F–fluoroazomycin–arabinoside (^{18}FAZA) PET in the setting of MRI guided adaptive radiotherapy in cervical cancer. *Acta Oncol* **49**(7): 941–7.

Segard T, Robins PD, Yusoff IF, Ee H, Morandeau L, Campbell EM, Francis RJ (2013) Detection of hypoxia with ^{18}F–fluoromisonidazole (^{18}F–FMISO) PET/CT in suspected or proven pancreatic cancer. *Clin Nucl Med* **38**(1): 1–6.

Semenza GL (2004) Hydroxylation of HIF–1: Oxygen sensing at the molecular level. *Physiology* **19**(4): 176–82.

Shi K, Souvatzoglou M, Astner ST, Vaupel P, Nüsslin F, Wilkens JJ, Ziegler SI (2010) Quantitative assessment of hypoxia kinetic models by a cross–study of dynamic ^{18}F–FAZA and ^{15}O–H2O in patients with head and neck tumors. *J Nucl Med* 2010; **51**(9): 1386–94.

Shibahara I, Kumabe T, Kanamori M, Saito R, Sonoda Y, Watanabe M, Iwata R, Higano S, Takanami K, Takai Y, Tominaga T (2010) Imaging of hypoxic lesions in patients with gliomas by using positron emission tomography with 1–(2–[^{18}F] fluoro–1–[hydroxymethyl]ethoxy) methyl–2–nitroimidazole, a new ^{18}F–labeled 2–nitroimidazole analog: Clinical article. *J Neurosurg* **113**(2): 358–68.

Souvatzoglou M, Grosu AL, Röper B, Krause BJ, Beck R, Reischl G, Picchio M, Machulla HJ, Wester HJ, Piert M (2007) Tumour hypoxia imaging with [^{18}F]FAZA PET in head and neck cancer patients: A pilot study. *Eur J Nucl Med Mol Imaging* **34**(10): 1566–75.

Swanson KR, Chakraborty G, Wang CH, Rockne R, Harpold HL, Muzi M, Adamsen TC, Krohn KA, Spence AM (2009) Complementary but distinct roles for MRI and ^{18}F–fluoromisonidazole PET in the assessment of human glioblastomas. *J Nucl Med*. **50**(1): 36–44.

Takahashi N, Fujibayashi Y, Yonekura Y, Welch MJ, Waki A, Tsuchida T, Sadato N, Sugimoto K, Itoh H (2000) Evaluation of [62]Cu labeled diacetyl–bis(N4–methylthiosemicarbazone) as a hypoxic tissue tracer in patients with lung cancer. *Ann Nucl Med* **14**(5): 323–8.

Tateishi K, Tateishi U, Sato M, Yamanaka S, Kanno H, Murata H, Inoue T, Kawahara N (2013) Application of ^{62}Cu–diacetyl–bis (N4– methylthiosemicarbazone) PET imaging to predict highly malignant tumor grades and hypoxia–inducible factor–1a expression in patients with glioma. *Am J Neuroradiol* 2013; **34**(1): 92–9.

Thorwarth D, Eschmann SM, Scheiderbauer J, Paulsen F, Alber M (2005) Kinetic analysis of dynamic ^{18}F–fluoromisonidazole PET correlates with radiation treatment outcome in head–and–neck cancer. *BMC Cancer*; **5**: 152.

Thorwarth D, Eschmann SM, Holzner F, Paulsen F, Alber M (2006) Combined uptake of [^{18}F]FDG and [^{18}F]FMISO correlates with radiation therapy outcome in head–and–neck cancer patients. *Radiother Oncol* **80**(2): 151–6.

Thureau S, Chaumet–Riffaud P, Modzelewski R, Fernandez P, Tessonnier L, Vervueren L, Cachin F, Berriolo-Riedinger A, Olivier P, Kolesnikov-Gauthier H, Blagosklonov O, Bridji B, Devillers A, Collombier L, Courbon F, Gremillet E, Houzard C, Caignon JM, Roux J, Aide N, Brenot-Rossi I, Doyeux K, Dubray B, Vera P (2013) Interobserver agreement of qualitative analysis and tumor delineation of ^{18}F–fluoromisonidazole and 3'–deoxy–3'–^{18}F–fluorothymidine PET images in lung cancer. *J Nucl Med* **54**(9): 1543–50.

Trinkaus ME, Blum R, Rischin D, Callahan J, Bressel M, Segard T, Roselt P, Eu P, Binns D, MacManus MP, Ball D, Hicks RJ (2013) Imaging of hypoxia with ^{18}F–FAZA PET in patients with locally advanced non–small cell lung cancer treated with definitive chemoradiotherapy. *J Med Imaging Radiat Oncol* **57**(4): 475–81.

Valk PE, Mathis CA, Prados MD, Gilbert JC, Budinger TF (1992) Hypoxia in human gliomas: Demonstration by PET with fluorine–18–fluoromisonidazole. *J Nucl Med* 1992; **33**(12): 2133–7.

Vaupel P, Harrison L (2004) Tumor hypoxia: Causative factors, compensatory mechanisms, and cellular response. *Oncologist* **9** (Suppl 5): 4–9.

Vera P, Bohn P, Edet–Sanson A, Salles A, Hapdey S, Gardin I, Ménard JF, Modzelewski R, Thiberville L, Dubray B (2011) Simultaneous positron emission tomography (PET) assessment of metabolism with ^{18}F–fluoro–2–deoxy–d–glucose (FDG), proliferation with ^{18}F–fluoro–thymidine (FLT), and hypoxia with ^{18}F–fluoro–misonidazole (F–miso) before and during radiotherapy in patients with non–small–cell lung cancer (NSCLC): A pilot study. *Radiother Oncol* **98**(1): 109–16.

Vercellino L, Groheux D, Thoury A, Delord M, Schlageter MH, Delpech Y, Barré E, Baruch-Hennequin V, Tylski P, Homyrda L, Walker F, Barranger E, Hindié E (2012). Hypoxia imaging of uterine cervix carcinoma with ^{18}F–FETNIM PET/CT. *Clin Nucl Med* **37**(11): 1065–8.

Wang K, Yorke E, Nehmeh SA, Humm JL, Ling CC (2009) Modeling acute and chronic hypoxia using serial images of ^{18}F–FMISO PET. *Med Phys* 2009; **36**(10): 4400–8.

Wilson WR, Hay MP (2011) Targeting hypoxia in cancer therapy. *Nat Rev Cancer* **11**(6): 393–410.

Yamane T, Kikuchi M, Shinohara S, Senda M (2011) Reduction of [^{18}F]fluoromisonidazole uptake after neoadjuvant chemotherapy for head and neck squamous cell carcinoma. *Mol Imaging Biol* **13**(2): 227–31.

Yue J, Yang Y, Cabrera AR, Sun X, Zhao S, Xie P, Zheng J, Ma L, Fu Z, Yu J (2012) Measuring tumor hypoxia with ^{18}F–FETNIM PET in esophageal squamous cell carcinoma: a pilot clinical study. *Dis Esophagus* **25**(1): 54–61.

Zegers CML, Van Elmpt W, Wierts R, Reymen B, Sharifi H, Öllers MC, Hoebers F, Troost EG, Wanders R, van Baardwijk A, Brans B, Eriksson J, Windhorst B, Mottaghy FM, De Ruysscher D, Lambin P (2013) Hypoxia imaging with [18F]HX4 PET in NSCLC patients: Defining optimal imaging parameters. *Radiother Oncol* **109**(1): 58–64.

Zimny M, Gagel B, DiMartino E, Hamacher K, Coenen HH, Westhofen M, Eble M, Buell U, Reinartz P (2006) FDG – A marker of tumour hypoxia? A comparison with [18F]–fluoromisonidazole and pO2–polarography in metastatic head and neck cancer. *Eur J Nucl Med Mol Imaging* **33**(12): 1426–31.

Table 1: Characteristics of the ideal hypoxia tracer

1	Hypoxia-specific retained in regions with low pO_2 levels, but not by normoxic or necrotic cells
2	Mechanism of cellular retention should be well defined and cell type independent
3	Sufficiently lipophilic to enter cells and allow uniform tissue distribution, but also sufficiently hydrophilic to avoid membrane sequestration, and have faster clearance from systemic circulation and normoxic tissue.
4	Pharmacokinetic profile and tissue distribution should exhibit little dependence on parameters that may co-vary with hypoxia, such as blood flow or pH.
5	High stability against non-hypoxia specific metabolism *in vivo*
6	Tissue kinetics should be suitable to imaging within a timeframe permitted in the clinical setting
7	Should be easy to synthesize and readily available.
8	Amenable dosimetry profile.
9	Be repeatable to allow both detection of hypoxia and return to normoxia
10	Should be effective in multiple tumour types.

pO_2: partial oxygen pressure (mmHg)

Table 2: Clinical hypoxia studies with PET in tumours.

Reference	Tracer	Tumour type(s)	N	Tracer retention (TBR; SUV)	Results
Valk *et al* 1992	^{18}F–FMISO	Brain	3	T:P: 0·71–1·49 at 120 min p.i.	^{18}F–FMISO–PET is a feasible method for detecting hypoxia in gliomas
Bruehlmyer *et al* 2004	^{18}F–FMISO	Brain	11	T:B: 0·96–2·07 At 90 min & ≥170 min p.i.	Increased ^{18}F–FMISO T:B observed in all tumours. T:B independent of tumour perfusion at later imaging times
Cher *et al* 2006	^{18}F–FMISO	Brain	17	– Static scan at 120 min p.i.	^{18}F–FMISO uptake in high grade, but not low grade, gliomas. Correlation between ^{18}F–FDG or ^{18}F–FMISO uptake with Ki67 and VEGFR–1 expression
Swanson *et al* 2009	^{18}F–FMISO	Brain	24	T:B$_{max,pre-therapy}$:2·7 T:B$_{max,post-therapy}$:1·7	Hypoxia volume generally straddled outer edge of the T1–Gd abnormality. Correlation between hypoxic volume and T1–Gd abnormality.[18]F–FMISO T:B reduced after therapy
Cheng *et al* 2013	^{18}F–FMISO	Breast	20	T:M$_{2h,Baseline}$: 0·72–3·07 T:M$_{4h,Baseline}$: 0·8–2·29 (16/20 patients) T:M$_{2h,Follow-up}$: 0·27–1·83 T:M$_{4h,Follow-up}$: 0·43–2·28 At 120 min & 180 min p.i. Hypoxia thresholds: T:M>1·2; SUV≥2·1	Correlation between FMISO uptake and endocrine therapy outcome. Poor correlation between FMISO uptake and HIF–1a immunostaining.
Gagel *et al* 2004	^{18}F–FMISO	H&N	16	T:M: 1·68 (range, 1·23–2·28) Av SUV$_{mean}$: 1·76; Av. SUV$_{max}$: 2·07 At 120 min p.i.	Average to high correlation between oxygen electrode and ^{18}F–FMISO T:M and SUV. No correlation between tumour oxygenation status and ^{18}F–FDG uptake
Hicks *et al* 2005	^{18}F–FMISO	H&N	15	SUV$_{max}$ Tumour: 2·5±0·5 Nodes: 2·3±0·5 At 120 min p.i.	Positive ^{18}F–FMISO uptake in 13 patients. Qualitative decrease in ^{18}F–FMISO and ^{18}F–FDG uptake induced by therapy
Thorwarth *et al* 2005	^{18}F–FMISO	H&N	15	Median SUV$_{max}$: 2·25 (range, 1·36–4·04) at 120 min & 180 min p.i.	Different types of characteristic hypoxia–perfusion patterns identified in tumours

Rajendran et al 2006	^{18}F–FMISO	H&N	73	Mean T:B$_{max}$1·6±0·46	T:B and presence of nodes were strong independent predictors of survival
Richin et al 2006	^{18}F–FMISO	H&N	45	Independent hypoxic score Static scan at 120 min p.i.	Higher risk of locoregional failure in hypoxic tumours. Patients on tirapazamine had lower risk of locoregional failure
Thorwarth et al 2006	^{18}F–FMISO	H&N	12	SUV$_{max}$: 2·20 (range, 1·4–3·22) At 120 min and 240 min p.i Hypoxia definition: SUV>1·4	No correlation between ^{18}F–FDG and ^{18}F–FMISO SUV. Maximum ^{18}F–FMISO SUV showed borderline significance for stratifying patient group
Zimny et al 2006	^{18}F–FMISO	H&N	24	Normoxic T:M$_{mean}$1·4 Hypoxic T:M$_{mean}$: 1·8	^{18}F–FMISO T:M higher in hypoxic tumours (as detected with oxygen electrode).Moderate correlation between ^{18}F–FDG and ^{18}F–FMISO uptake.
Eschmann et al 2007	^{18}F–FMISO	H&N	14	SUV$_{mean, pre–therapy}$ 2·54±0·81 T:M$_{pre–therapy}$ 1·9±0·64 SUV$_{mean, post–therapy}$: 1·98±0·47, T:M$_{post–therapy}$: 1·49±0·26 At 240 min p.i. Hypoxia definition: T:M≥2 threshold	Radiotherapy decreased^{18}F–FMISO SUV and T:M ratio.
Gagel et al 2007	^{18}F–FMISO	H&N	38	SUV$_{mean}$: 1·69 SUV$_{max}$: 1·98 T:M$_{mean}$: 1·57 T:B$_{mean}$: 1·13	Moderate correlation between oxygen measurements and ^{18}F–FMISO uptake. Low correlation between ^{18}F–FDG and ^{18}F–FMISO
Lee et al 2008	^{18}F–FMISO	H&N	20	Static scan at 120–150 min p.i. Hypoxia definition: T:M≥1·3	Variable ^{18}F–FMISO distribution
Nehmeh et al 2008	^{18}F–FMISO	H&N	13	SUV 1·9–4·5 At 117–195 p.i. TBR≥1·2	Good correlations intra–tumour^{18}F–FMISO distributions in 6/13 patients, consistent with chronic hypoxia
Dirix et al 2009	^{18}F–FMISO	H&N	15	Hypoxic volume$_{pre–therapy}$ 4·1ml, T:B$_{max, pre–therapy}$: 1·5 Hypoxic volume$_{post–therapy}$: 0·3ml T:B$_{max,post–therapy}$: 1·2 at 120–160 min p.i Hypoxia definition: T:B>1·2	Disease free survival correlates negatively with baseline T:B$_{max}$ and initial hypoxic volume
Lee et al 2009	^{18}F–FMISO	H&N	28	–	Heterogeneous distribution of ^{18}F–FMISO noted in the primary and/or nodal disease in 90% of

				patients

Abolmaali *et al* 2011	^{18}F–FMISO	H&N	23	$SUV_{max,2h}$: 2·2 (range,1·3–3·4) $T:M_{2h}$: 1·46 $SUV_{max,4h}$: 2·4 (range,1·1–4·4) $T:M_{4h}$: 1·6	^{18}F–FMISO contrast increases 2h–4h p.i.
Kikuchi *et al* 2011	^{18}F–FMISO	H&N	17	Median SUV_{max}: 2·3 Median T:M: 1·3 At 150 min p.i. Hypoxia definition: 1·3	Disease specific survival was significantly lower in patient group with high basal ^{18}F–FMISO SUV_{max} and $T:M_{max}$
Yamane *et al* 2011	^{18}F–FMISO	H&N	13	$SUV_{max,pre–therapy}$2·2 (range, 0·7–3·6) $T:M_{,pre–therapy}$: 1·6 (range: 1·1–2·2). Responders: −18·7% SUV_{max}; −22·5% T:M; −82·65% hypoxic volume Non–responders: −5·5% SUV_{max} 10·2% T:M −8·8% hypoxic volume (−/+ denote % increase and decrease respectively) At 150 min p.i.	^{18}F–FMISO SUV_{max}, T:M and hypoxic volume significantly decreased after neo-adjuvant chemotherapy
Sato *et al* 2013	^{18}F–FMISO	H&N	23	Median SUV_{max}: 1·83 (range, 0·8–2·7) Median SUV_{max}: 16·5 (range, 1·0–32·3)	Weak significant correlation between ^{18}F–FMISO and ^{18}F–FDG SUV_{max}. ^{18}F–FMISO SUV_{max} was significantly higher in HIF–1α–positive cases than in HIF–1α–negative cases.
Okamoto *et al* 2013	^{18}F–FMISO	H&N	11	$SUV_{max,Baseline}$:3·16±1·29 $SUV_{max,48h}$: 3·02±1·12 $T:B_{Baseline}$: 2·98±0·83 $T:B_{48h}$: 2·97 ± 0·64 $T:M_{Baseline}$: 2·25 ± 0·71 $T:M_{48h}$: 2·19 ± 0·67 At 240 min p.i. Hypoxia threshold: T:B≥1·5; T:M≥1·25	High reproducibility between SUV, T:B, T:M and hypoxic volume measurements between the two ^{18}F–FMISO scans (baseline and at 48h)
Mortensen *et al* 2010	^{18}F–FMISO	H&N Sarcoma	19	$T:M_{med}$: H&N: 1·68 (range, 0·7–2·38) Sarcoma: 0·78 (range, 0·7–1)	No correlation between ^{18}F–FMISO retention and oxygen electrode
Koh *et al* 1995	^{18}F–FMISO	Lung	7	Static scan at 120–180p.i. TBR≥1·4 threshold to define hypoxia	Radiotherapy reduced median fractional hypoxic volume from 58% to 22%

Cherk *et al* 2006	^{18}F–FMISO	Lung	21	SUV: 0·4–2·14; T:N: 1·18–9·73 At 120 min p.i.	Low ^{18}F–FMISO uptake. Poor correlation between ^{18}F–FMISO and ^{18}F–FDG uptake
Gagel *et al* 2006	^{18}F–FMISO	Lung	8	$SUV_{mean, pre–therapy}$: 2·31 ± 0·2 $SUV_{max, pre–therapy}$: 2·77 ±0·27 $T:M_{pre–therapy}$: 1·99±0·49 $SUV_{mean, post–therapy}$: 1·83 ± 0·12 $SUV_{max, post–therapy}$:2·19±0·13 $T:M_{post–therapy}$: 1·36±0·08 At 180 min p.i.	^{18}F–FMISO can define hypoxic sub–regions. Changes in FMISO and ^{18}F–FDG PET measure early response to therapy.
Vera *et al* 2011 (22)	^{18}F–FMISO	Lung	5	$SUV_{max, pre–therapy}$: 1–2·5 $SUV_{max, post–therapy}$: 1–2·4	^{18}F–FMISO uptake higher in tumours than nodes and did not change during therapy
Thureau *et al* 2013	^{18}F–FMISO	Lung	10	–	Low reproducibility and inter–observer agreement for ^{18}F–FMISO volume measurements on the basis of visual scoring. T:M≥1·4 recommended for hypoxic volume delineation.
Segard *et al* 2013	^{18}F–FMISO	Pancreatic	10	Mean SUV_{max}: 2·3 (range, 1–3·4)	^{18}F–FMISO accumulation observed in 2/10 patients on the basis of visual analysis. Minimal ^{18}F–FMISO accumulation in pancreatic tumours; correlation with other imaging modalities required to allow tumour localization and semi–quantitative analysis.
Hugonet *et al* 2011	^{18}F–FMISO	Renal	53	Static scan at 120 min p.i. Hypoxia definition: TBR>1·2	Reduction in hypoxic volume post–therapy.
Roels *et al* 2008	^{18}F–FMISO	Rectal	15		Mismatch between ^{18}F–FDG and ^{18}F–FMISO scans.[18]F–FMISO uptake reduced after therapy
Bentzen *et al* 2003	^{18}F–FMISO	Sarcoma	13	T:M <1–1·6	^{18}F–FMISO accumulation observed in 2/7 malignant tumours. No correlation between ^{18}F–FMISO and pO_2 measurements
Rajendran *et al* 2003	^{18}F–FMISO	Sarcoma	19	$T:B_{max}$ 1·10–3·46 At 120 min p.i. TBR≥1·2 to define hypoxia	^{18}F–FMISO uptake observed in 14 patients. Poor correlation between tumour grade, hypoxia volume and ^{18}F–FDG T:B.

Study	Tracer	Tumour type	n	Uptake values	Findings
Rajendran *et al* 2004	^{18}F–FMISO	Brain Breast H&N Sarcoma	49	T:B$_{max}$: Brain 2·43 (range, 1·7–2·9) Breast 1·52 (range, 0·93–2·6) H&N: 1·5 (range, 0·88–2·4) Sarcoma: 1·46 (range, 1·1–2·1)	Hypoxia detected in all tumour types. Low correlation between glucose metabolism and hypoxia
Schuetz *et al* 2010	^{18}F–FAZA	Cervical	15	T:M$_{max}$: 1·2–3·6 At 60 min & 120 min p.i.	5/15 patients had visually identifiable tumours.
Grosu *et al* 2007	^{18}F–FAZA	H&N	18	T:M$_{mean}$: 1·6 T:M$_{max}$: 2 At 120 min p.i. Hypoxia threshold: SUV≥1·5	^{18}F–FAZA uptake located in single confluent region in 11/18 patients and as multiple diffuse regions in 4/18 patients
Souvatzoglou *et al* 2007	^{18}F–FAZA	H&N	11	SUV$_{max}$: 2·3 (range, 1·5–3·4) SUV$_{mean}$: 1·4 (range, 1–2·1) T:M: 2 (range, 1·6–2·4)	T:M ratio increased 60min post injection. ll tumours had T:M>1·5· Tumour volume with T:M>1·5 was highly variable
Mourtensen *et al* 2011	^{18}F–FAZA	H&N	40	Median T:M$_{max}$1·5 At 120 min p.i. Hypoxia threshold: ≥ 1·4	High uptake associated with lower disease–free survival. Radiotherapy treatment reduced hypoxic volume
Bollineni *et al* 2013	^{18}F–FAZA	Lung	11	Median T:B : 2·8 (range, 1·8–4·6) T:B≥1·2 for hypoxic volume definition.	Not significant correlation between ^{18}F–FAZA T:B and ^{18}F–FDG SUV$_{max}$ or lesion size. Heterogeneous intra–tumoural distribution for ^{18}F–FAZA based visual analysis.^{18}F–FAZA PET is able to detect heterogeneous distributions of hypoxic sub–volumes.
Trinkhaus *et al* 2013	^{18}F–FAZA	Lung	17	–	11/17 patients had baseline hypoxia based on qualitative assessment. 6/8 patients with scans following chemoradiation had resolution of hypoxia on the basis of qualitative analysis.
Garcia–Parra *et al* 2011	^{18}F–FAZA	Prostate	14	T:N$_{mean}$: 1·21	^{18}F–FAZA uptake not increased in tumours. No evidence of hypoxia as assessed by CaIX IHC staining
Havelund *et al* 2013	^{18}F–FAZA	Rectal	14	T:M$_{mean}$: 2·83	^{18}F–FAZA–PET is feasible for visualization of hypoxia in rectal cancer.
Postema *et al* 2009	^{18}F–FAZA	H&N Lung Lymphoma Glioma	50	H&N TBR : 1·2–2·7; SUV$_{max}$1·05–2·35 Lung TBR : 1·3–3·7; SUV$_{max}$0·81–1·93 Lymphoma TBR: 1·2–3; SUV$_{max}$1·07–	High TBR in all 7 gliomas; high TBR, SUV$_{max}$ observed in 6/9 H&N tumours; moderate TBR, SUV$_{max}$ in 3/21 lymphomas;

				4·52 Glioma TBR : 1·9–15·6 At 120–180 min p.i.	increased TBR, SUV_{max} in 7/11 lung patients
Lethiö *et al* 2001	^{18}F–FETNIM	H&N	8	T:M_{max} 1–4 at 3h p.i.	Tumour distribution volume correlated strongly with ^{18}F–FETNIM SUV between 60 and 120 min p.i. and blood flow, but not with ^{18}F–FDG SUV. Values compare favourably with ^{18}F–FMISO data. Late time–point ^{18}F–FETNIM T:M are indicative of hypoxia.
Lethiö *et al* 2003	^{18}F–FETNIM	H&N	10	Median T:M: 1·41 (range, 0·86–2) Median T:P_{mean}: 0·96 (range, 0·74–1·1) Median T:P_{max}: 1·29 (range, 0·91–1·98)	T:P is good estimate of tumour hypoxia
Lethiö *et al* 2004	^{18}F–FETNIM	H&N	21	Median T:P_{max} : 1·10 (range, 0·81–1·98) T:P>0·93 used for hypoxic volume definition	Patients with higher fractional hypoxic volumes and T:P correlated with poorer survival.
Hu *et al* 2010	^{18}F–FETNIM	Lung	42	$SUV_{max,Tumour}$: 2·43 $SUV_{max,Normal}$: 0·87 T:N: 2·48 at 120 min p.i.	SUV_{max} higher in tumours than normal tissue. Similar data observed at 60 and 120 min p.i.
Li *et al* 2010	^{18}F–FETNIM	Lung	26	–	^{18}F–FETNIM T:B ratio and hypoxic volume were strong predictors for overall survival. No correlation between ^{18}F–FETNIM and ^{18}F–FDG uptake
Vercellino *et al* 2012	^{18}F–FETNIM	Cervical	16	T:M : 1·3–5·4	High uptake associated with lower progression free and overall survival
Yue *et al* 2012	^{18}F–FETNIM	Oesophageal	28	$SUV_{max, complete\ response}$: 3·2 $SUV_{mean, complete\ response}$: 2·1 $SUV_{max, partial\ response}$: 4·5 $SUV_{mean, partial\ response}$: 2·9 $SUV_{max, stable\ disease}$: 5·9 $SUV_{mean, stable\ disease}$: 3·2 Threshold for hypoxia SUV_{max}:$SUV_{mean,spleen}$: 1·3	SUV_{max}, SUV_{mean} are reproducible. High baseline SUV_{max} associated with poor clinical response
Zegers *et al* 2013	^{18}F–HX4	Lung	15	$SUV_{max,2h}$: 1·47 ± 0·36 $SUV_{max,4h}$: 1·34 ± 0·37 T:$B_{max,2h}$: 1·56 ± 0·30 T:$B_{max,2h}$: 2·03 ± 0·55	T:B_{max}>1·4 at 240 min p.i. was observed in 80% of the primary tumours and 60% of lymph node regions. T:B_{max} increased over acquisition time, although pattern

				at 240 min p.i Hypoxia threshold: T:B>1·4	stabilized between 120–180 min p.i.
Kaneta 2007	^{18}F–FRP170	Normal Lung	4/3	T:M$_{1h}$: 1·69 T:B$_{1h}$: 1·09 T:M$_{2h}$: 1·96 T:B$_{2h}$: 1·24 at 120 min p.i	T:B stable at 60–120 min p.i. Images obtained 60 min p.i. may allow evaluation of tumour accumulation in a clinical setting
Shibahara *et al* 2010	^{18}F–FRP170	Brain	8	SUV$_{max}$: 1·3–2·3	SUV$_{max}$ correlated positively with HIF–1a immunostaining.
Beppu *et al* 2013	^{18}F–FRP170	Brain	12	SUV$_{mean, Tumour}$: 1·58±0·35 SUV$_{mean, Normal}$: 0·82±0·16 T:N : 1·95±0·33	Significant correlation between T:N, pO2, and strong nuclear immunostaining for HIF–1α in areas of high 18F–FRP170 accumulation 60 min p.i in glioblastoma patients.
Dehdashti *et al* 2004	^{60}Cu–ATSM	Cervical	14	Mean T:M 3·4±2·8	Tumour uptake of ^{60}Cu–ATSM inversely related to progression–free survival and overall survival. No correlation between FDG and ^{60}Cu–ATSM uptake
Grigsby *et al* 2007	^{60}Cu–ATSM	Cervical	15	–	4 year overall survival estimates were 75% for patients with non–hypoxic tumours and 33% for those with hypoxic tumours. Overexpression of VEGF, EGFR, COX2, CAIX and increased apoptosis observed in hypoxic tumours.
Dehdashti *et al* 2008	^{60}Cu–ATSM	Cervical	38	T:M 3·8±2·0	Tumour uptake of ^{60}Cu–ATSM was inversely related to progression–free survival and cause–specific survival. 3 year progression free survival of patients with non–hypoxic tumours was 71%, and 28% for those with hypoxic tumours
Minagawa *et al* 2011	^{62}Cu–ATSM	H&N	15	Mean SUV$_{max}$5·5±1·7	All 5 patients with SUV$_{max}$<5 were complete responders
Dehdashti *et al* 2003	^{60}Cu–ATSM	Lung	19	Mean T:M$_{pre–therapy}$2·3±1 Mean SUV$_{mean, pre–therapy}$:3·2±1 Responders: Mean T:M$_{pre–therapy}$: 1·5 Non–responders: Mean T:M$_{pre–therapy}$: 3·4	Imaging with ^{60}Cu–ATSM feasible in NSCLC. Mean T:M lower in responders than non–responders. Mean SUV not different between these groups

Dietz *et al* 2008	^{60}Cu–ATSM	Rectal	19	Mean T:M 2·5±0·9 At 30–60 min p.i. Hypoxia threshold: T:M>2·6	Median tumour–to–muscle activity ratio of 2·6 discriminated those with worse prognosis from those with better prognosis. Overall and progression–free survival worse in hypoxic tumours
Lolith *et al* 2009	^{62}Cu–ATSM	Lung	13	$SUV_{mean, SCC}$: 1·95±0·88 $SUV_{mean, Adenocarcinoma}$: 1·54±0·92 At 30 min & 60 min p.i.	^{18}F–FDG and ^{62}Cu–ATSM had spatially similar distributions in adenocarcinomas

Note: N= number of patients; T:M: tumour–to–muscle ratio; T:P: tumour–to–plasma ratio; T:B: tumour–to blood ratio; T:N: tumour–to–normal–tissue ratio; TBR: tumour–to–background ratio; SUV: standardized uptake value; pO_2: partial oxygen pressure; p.i.:post injection; VEGFR: vascular endothelial growth factor; EGFR: epidermal growth factor; CAIX: carbonic anhydrase IX; H&N: head and neck cancer, NSCLC: non–small cell lung cancer; RT: radiotherapy

Tumor type	^{18}F-FMISO	^{18}F-HX4	^{18}F-FAZA	^{18}F-FETNIM	^{18}F-EF5	^{18}F-FRP170	Cu-ATSM
Brain	Yes	Not recommended	Yes		Recommended	Yes	Recommended
Head & Neck	Yes	Yes	Yes	Yes	Yes		Yes
Breast	Yes						
Sarcoma	Variable data						
Lung	Yes	Yes	Yes	Yes		Yes	Yes
Lymphoma			Yes				
Renal	Variable data Not recommended	Not recommended	Not recommended	Not recommended	Not recommended		Recommended
Liver	Not recommended	Recommended		Not recommended	Not recommended		Not recommended
Colorectal	No Not recommended		Yes	Not recommended	Not recommended		Yes
Bladder	Not recommended	Not recommended	Not recommended	Not recommended	Not recommended		Recommended
Cervical			Yes	Yes			Yes
Prostate			No				Not recommended

Table 3: Matrix summarising clinical imaging findings with leading hypoxia tracers

Titles and legends to figures

Figure 1: Structures and logP values of PET hypoxia radiotracers. The logP value (partition coefficient) of each radiotracer is shown in the parentheses. Positive logP values indicate a lipophilic molecule, whereas negative logP values represent a hydrophilic molecule.

Figure 2: Tumour-to-reference-tissue ratios and range in different tumour sites for the PET hypoxia tracers discussed in this review. For nitroimidazole-based analogues (FMISO, FAZA, FETNIM, HX4, FRP-170) values are given for acquisitions performed at 120 min post tracer administration. For Cu-ATSM values are presented for scans conducted 60 min.

Figure 3: (a) Transverse ^{18}F-FMISO fused PET/CT overlay image acquired at baseline of a patient with metastatic renal cell carcinoma (mRCC) in the neck acquired at 2.5-3h p.i (image courtesy of Professors Tim Eisen and Duncan Jodrell, University of Cambridge, UK) (b) ^{64}Cu-ATSM fused PET/CT overlay image of a patient with advanced laryngeal squamous cell carcinoma (LSCC) at 80-90 min p.i. The transverse slice includes primary tumour and local lymph node (image courtesy of Dr Anastasia Chalkidou, King's College London, UK)
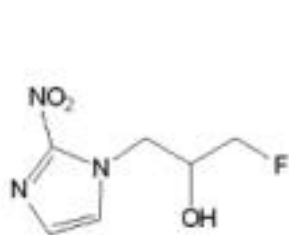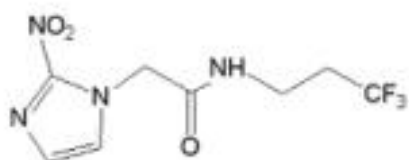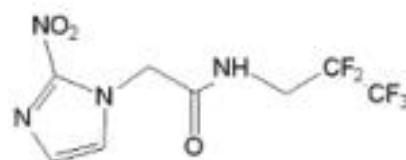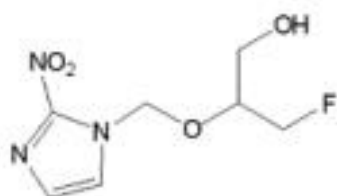
FMISO (logP: 0.4)
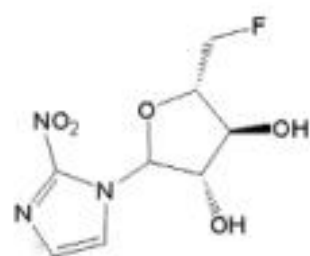
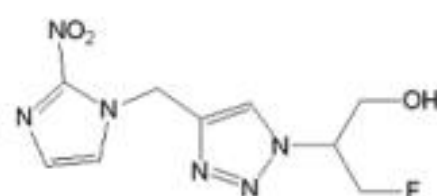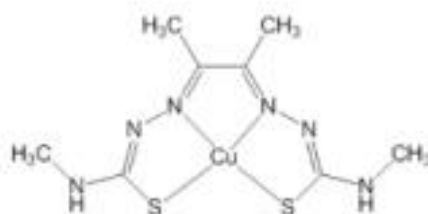FAZA (logP: -0.4)
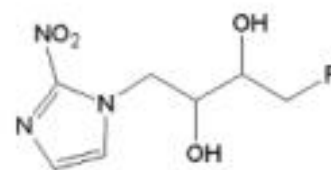
FETNIM (logP: -0.77)

EF3 (logP: 0.05)

EF5 (logP: 0.6)

FRP-170 (logP: 0.094)

HX4 (logP: -0.69)

Cu-ATSM (logP: 1.48)